J. Fluid Mech. (2015), *vol.* 779, *pp.* 309–324.
doi:10.1017/jfm.2015.389

Local scour around structures and the phenomenology of turbulence

Costantino Manes[1,†] **and Maurizio Brocchini**[2]

[1]Faculty of Engineering and the Environment, University of Southampton, Southampton SO17 1BJ, UK

[2]Dipartimento ICEA, Università Politecnica delle Marche, via Brecce Bianche 12, 60131 Ancona, Italy

(Received 2 October 2014; revised 24 June 2015; accepted 3 July 2015;
first published online 14 August 2015)

The scaling of the scour depth of equilibrium at the base of a solid cylinder immersed within an erodible granular bed and impinged by a turbulent shear flow is investigated here, for the first time, by means of the phenomenological theory of turbulence. The proposed theory allows the derivation of a predictive formula that (i) includes all the relevant non-dimensional parameters controlling the process, and (ii) contrary to commonly employed empirical formulae, is free from scale issues. Theoretical predictions agree very well with experimental data, shed light on unresolved issues on the physics of the problem, and clarify the effects of various dimensionless parameters controlling the scouring process.

Key words: hydraulics, sediment transport, turbulence theory

1. Introduction

In this paper we investigate the local scour around cylindrical elements inserted within a granular bed and piercing the free surface of open channel shear flows (figure 1). Quantifying the maximum depth of the scour hole generated at these conditions is relevant to a wide range of engineering applications, including the design and risk assessment of hydraulic structures such as bridge piers, off-shore platforms and wind turbines. The problem can be stated as follows: for a given structure (e.g. shape and orientation with respect to the flow), some arbitrarily chosen extreme flow conditions and sediment size, what is the maximum depth of the scour hole forming around the foundations? The enormous amount of research carried out to give an answer to this question led to the development of many predictive formulae derived through empirical approaches, which traditionally rely on dimensional analysis and data fitting to find functional relations between non-dimensional groups (Melville & Coleman 2000; Ettema, Constantinescu & Melville 2011). This approach has two main shortcomings. First, data are obtained mainly from laboratory experiments, which suffer from scale issues and, in turn, hide the real shape of functional relations between non-dimensional groups at field scales. Second, even when reliable large-scale experiments are available, the empirical approach does not provide a theoretical framework to interpret the experimental data and to understand the physics underlying such functional relations. As a result, currently available formulae are

† Email address for correspondence: c.manes@soton.ac.uk

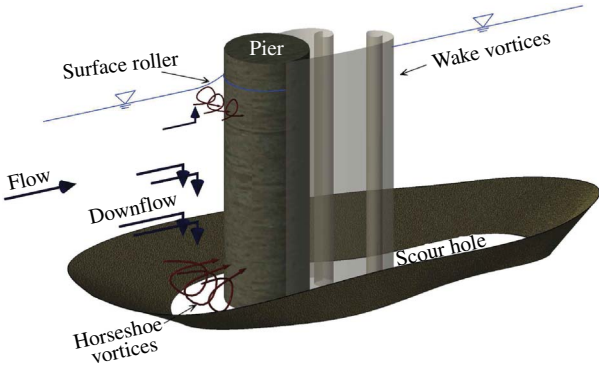

FIGURE 1. (Colour online) Sketch of eddies and scour geometry induced by an open channel shear flow impinging on a cylindrical element inserted within an erodible bed.

affected by large uncertainties and the physics of local scour phenomena occurring around structures is far from being understood. We argue that, although the empirical approach has provided an important guide to quantifying local scour for practical applications, future advances in this research area may benefit from the development of methodologies that are founded more on physical than empirical grounds. To this end we propose a new formula to predict scour depths, which is derived by merging theoretical aspects (i.e. the phenomenological theory of turbulence) with empirical observations. The proposed approach is scale-independent and clarifies the effects of various dimensionless groups on local scour processes. We focus on the simplified case of a cylindrical structure with circular cross-section, because it represents the traditional template for studying scour processes around structures and because it finds important applications in civil and off-shore engineering.

The paper is organized as follows: § 2 provides the theoretical derivation of scour predictive formulae; in § 3 experimental data taken from the literature are used to validate theoretical predictions; § 4 is devoted to the final discussion and the conclusions.

2. Theory

2.1. *General aspects*

When an open channel flow impinges upon a cylindrical rigid structure, turbulence is generated in the form of a horseshoe vortex, a wake vortex and a surface roller (figure 1). The horseshoe vortex is the main factor for sediment entrainment since it causes a significant increase in the shear stress around the base of the structure. The wake vortex contributes to lifting the entrained sediment and displacing it outside the scour hole. The surface roller (i.e. a recirculating mass of turbulent water) develops near the free surface due to the formation of a bow wave. The influence of the surface roller on scouring is significant only at shallow flow conditions, namely when the flow depth is smaller than or comparable to the pier width (Melville & Coleman 2000; Ettema *et al.* 2011).

Local scouring can occur in so-called clear-water or live-bed conditions depending on whether sediment transport occurs upstream of the cylinder. In both cases local scour is triggered by the horseshoe vortex at the base of the cylinder, provided that local shear stresses exceed the critical shear stress of the sediment (Ettema

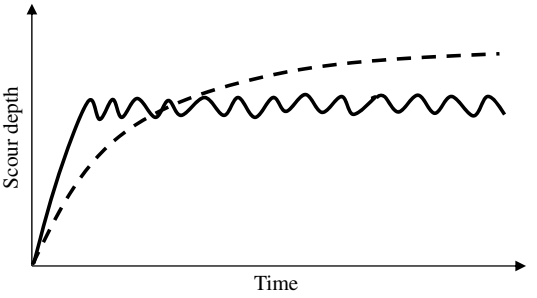

FIGURE 2. Conceptual description of the scour evolution in time for clear-water (dashed line) and live-bed (solid line) conditions.

et al. 2011). As the scour hole deepens, the erosive strength of the horseshoe vortex decreases until an equilibrium condition is reached. In the clear-water case such an equilibrium is reached when the shear stress at the base of the scour-hole approaches the critical shear stress associated with the sediment lying on the river bed. In live-bed conditions, instead, equilibrium conditions are dictated by a balance between ingoing and outgoing sediment fluxes (Melville 1984). In both cases the vertical distance between the undisturbed bed level and the deepest point within the scour hole is commonly defined as the equilibrium scour depth (i.e. y_s).

Figure 2 illustrates the typical evolution in time of the scour depth observed in live-bed and clear-water laboratory experiments. In live-bed conditions, equilibrium is reached very rapidly and y_s oscillates due to the passage of bed-forms. In clear-water conditions the concept of equilibrium is not clear and is still a matter of controversy (Lança *et al.* 2013). Some authors support the concept that equilibrium is reached in an arbitrarily defined finite time (Melville & Chiew 1999; Kothyari, Hager & Oliveto 2007), whereas others argue that equilibrium can be reached only asymptotically and suggest that y_s should be estimated by extrapolation of scour curves (like those reported in figure 2) at a time equal to infinity (Sheppard, Odeh & Glasser 2004; Lança *et al.* 2013). Lança *et al.* (2013) report that for identical experimental conditions y_s can vary by 10–20 % depending on how it is defined, so care must be taken when comparing results from different experiments. We come back to this issue in § 3.

2.2. *Clear-water conditions*

In clear-water conditions, provided that the ratio between the depth-averaged velocity in the undisturbed channel (i.e. V_1) and the sediment critical velocity is high enough (say $0.5 \leqslant V_1/V_c \leqslant 1$, where V_c is the sediment critical velocity, which depends on both sediment diameter and flow depth), the horseshoe vortex erodes the sediment at the base of the structure until the shear stress generated within the scour hole approaches the critical shear stress value (Ettema *et al.* 2011) and equilibrium conditions are reached. The point of maximum scour depth is normally located at the base of the scour hole in close proximity to the cylinder, either at its upstream face or at its flanks (Ettema *et al.* 2011). After careful examination of the results from experiments and numerical simulations presented in the literature, we argue that the local slope of the sediment bed near the point of maximum depth is consistently zero (Unger & Hager 2007; Kirkil, Constantinescu & Ettema 2008; Ettema *et al.* 2011). Therefore, at this

location, the critical shear stress of the sediment (i.e. τ_c) is presumably independent of local-slope (i.e. gravitational) effects and, assuming that the flow within the scour hole is in the fully rough regime (i.e. turbulence around the pier is fully developed and momentum transfer at the sediment–water interface is weakly influenced by viscosity), equilibrium conditions can be mathematically expressed as (Shields 1936)

$$\tau \leqslant \tau_c \sim (\rho_s - \rho)\, gd, \tag{2.1}$$

where τ is the shear stress at the point where the maximum scour depth occurs, ρ_s is the density of the sediment material, ρ is the density of the fluid, g is the gravity acceleration, d is the characteristic sediment diameter and the $\sim$ symbol means 'scales as'.

We now aim to derive a simple analytical formula that links the scour depth of equilibrium with easily measurable properties of the impinging flow, the sediment bed and the geometry of the cylindrical structure. The following derivation is inspired by the work of Gioia & Bombardelli (2005) and Bombardelli & Gioia (2006), who have used an approach based on the phenomenology of fully developed turbulence (see e.g. Frisch 1995) to investigate local scouring induced by turbulent jets.

Following Frisch (1995), the phenomenology of fully developed turbulence can be considered as a shorthand system that can be used to recover Kolmogorov's scaling laws (Kolmogorov 1991), which were originally derived in a much more systematic and (perhaps) rigorous way. In the present paper we make use of Kolmogorov's theory of turbulence to derive an expression for τ that results from the interaction between large- and small-scale eddies impinging the scour-hole surface.

We start by recalling two important paradigms of turbulence phenomenology. (i) For fully developed turbulent flows, the turbulent kinetic energy (TKE) per unit mass is injected into the flow at scales commensurate with the largest eddies and is independent of viscosity. (ii) TKE, introduced at a rate ϵ, cascades from large to small scales at the same rate until eddies of sufficiently small scale dissipate it into internal energy still at the same rate ϵ. Following Kolmogorov's theory (Kolmogorov 1991), the length scale at which the energy cascade begins to be influenced by viscosity is $\eta = (\nu^3/\epsilon)^{1/4}$, where η is the Kolmogorov length scale. Since TKE production occurs at large scales and is independent of viscosity, dimensional arguments suggest that $\epsilon \sim V^3/S$, where V and S are the characteristic velocity and length scale of large eddies. At scales l that are much smaller than S but also much larger than η (i.e. scales contained within the so-called inertial range), the energy cascade occurs inviscidly and $\epsilon \sim V^3/S \sim u_l^3/l$, where u_l is the characteristic velocity of eddies of size l. This implies that

$$u_l \sim V \left(\frac{l}{S}\right)^{1/3}, \tag{2.2}$$

which is a well-known result of Kolmogorov's theory of turbulence (Frisch 1995).

We can now go back to the turbulent flow generated within the scour hole forming at the base of a cylindrical structure. Under fully developed turbulence conditions and neglecting viscous components, the shear stress τ acting on the scour surface formed by sediment grains of diameter d is the Reynolds stress $\tau = \rho\overline{u'w'}$, where u' and w' are defined as the velocity fluctuations parallel and normal to the mean flow direction, respectively, and the over-bar identifies turbulence-averaging (figure 3).

Provided that d belongs to the inertial range of scales (i.e. $\eta \ll d \ll S$), Gioia & Bombardelli (2005) argue that eddies of size much larger than d can hardly contribute to w' because they are too large to exchange momentum in the fluid space between

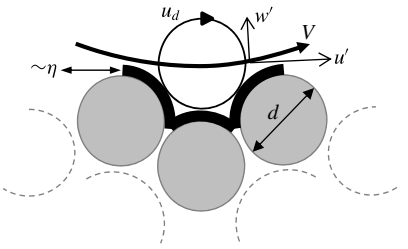

FIGURE 3. Schematic representation of the interaction between large-scale eddies and eddies scaling with the sediment diameter d. V is the characteristic velocity of large-scale eddies (i.e. eddies scaling with S) and u_d is the characteristic velocity of near-bed eddies (i.e. eddies scaling with the sediment diameter d); u' and w' are velocity fluctuations along and normal to the main flow direction respectively; η is the Kolmogorov length scale that quantifies the thickness of the viscous sublayer (Gioia & Chakraborty 2006), as discussed in § 3.

two successive roughness elements. In contrast, eddies of size smaller than d do fit within this space but are associated with lower characteristic velocities (i.e. recall Kolmogorov's scaling $u_l \sim V(l/S)^{1/3}$). This implies that w' is dominated by eddies of size d. Conversely, u' is influenced by the whole spectrum of turbulence length scales and therefore u' is dominated by V. Therefore, the shear stress scales as $\tau \sim \rho u_d V$, where $u_d \sim V(d/S)^{1/3}$, and hence

$$\tau \sim \rho V^2 \left(\frac{d}{S}\right)^{1/3}. \tag{2.3}$$

Strictly speaking, Kolmogorov's scaling (as applied in deriving the expression above) is valid if small-scale turbulence is homogeneous and isotropic. Turbulent flows within scour holes and near the sediment–water interface may not display these properties because of the significant strain rates of the mean flow imposed by the presence of the scour hole and the cylinder themselves. Nonetheless, the literature suggests that Kolmogorov's predictions still hold for non-homogeneous and anisotropic flows (Knight & Sirovich 1990; Moser 1993). Moreover, Saddoughi & Veeravalli (1994) and Saddoughi (1997) show that for wall-bounded flows the energy spectra display Kolmogorov scaling across a range of wavenumbers at which local isotropy is not strictly valid, and this was observed in both equilibrium (i.e. canonical turbulent boundary layers) and non-equilibrium flows (i.e. flows characterized by complex mean strain rates as in the case of flows around a cylinder). Finally, Gioia and co-workers show that applying Kolmogorov's scaling to the description of turbulent flows in close proximity to rough and smooth boundaries (these include near-wall flows in pipes and channels where turbulence is neither homogeneous nor isotropic) allows the recovery of many important empirical relations pertaining to classical hydraulics (Gioia & Bombardelli 2002; Gioia & Chakraborty 2006). It is therefore suggested that the validity of the phenomenological theory of turbulence (in the sense of Kolmogorov) to describe small-scale turbulence within a scour hole is, at least, a plausible hypothesis.

It is now assumed that the characteristic length scale of the energetic eddies forming within the scour hole (i.e. presumably the characteristic length scale of the horseshoe vortex) approximates the depth of the scour hole itself. This means that at equilibrium

conditions it is $S \sim y_s$, where y_s is the scour depth of equilibrium. This is a reasonable assumption because at equilibrium conditions, the horseshoe vortex is notoriously fully buried within the scour hole, as reported by Unger & Hager (2007) and Kirkil *et al.* (2008).

Computing τ requires us to find a scaling formula for V, which is derived following energetic principles. We recall that ϵ scales as $\epsilon \sim V^3/S$. However, ϵ can also be estimated as the power associated with large-scale eddies (i.e. P) divided by the mass of the fluid contained within their characteristic volume, i.e. $\epsilon = P/M$. P can be estimated as the work of a drag force F acting on the cylinder against the mean flow and, hence, as $P = FV_1$, where V_1 can be taken as the depth-averaged velocity of the approaching flow. The drag force can thus be computed as $0.5\rho C_d a S V_1^2$, where C_d is a drag coefficient, a is the cylinder diameter, and aS is the frontal area of the cylinder exposed to scouring. The power of the localized turbulent eddies is estimated from the drag force acting on the exposed portion of the cylinder because, presumably, wake eddies forming above it do not contribute to the scour process.

From dimensional considerations, the mass of the characteristic large-scale eddy can be computed as $M \sim \rho S^3$. This implies that

$$\epsilon = \frac{P}{M} \sim \frac{C_d a V_1^3}{S^2} \sim \frac{V^3}{S} \tag{2.4}$$

and hence

$$V \sim V_1 \left(\frac{C_d a}{S}\right)^{1/3}. \tag{2.5}$$

Combining (2.3) and (2.5) leads to

$$\tau \sim \rho V_1^2 \left(\frac{C_d a}{S}\right)^{2/3} \left(\frac{d}{S}\right)^{1/3}. \tag{2.6}$$

When the scour process reaches equilibrium the sediment stops moving, and the shear stress approaches the value of the critical shear stress (i.e. incipient motion conditions, $\tau \approx \tau_c$), and hence, after some algebra,

$$S \sim y_s \sim \left(\frac{V_1^2}{g}\right) \left(\frac{\rho}{\rho_s - \rho}\right) (C_d)^{2/3} \left(\frac{a}{d}\right)^{2/3} \tag{2.7}$$

or, alternatively,

$$\frac{y_s g}{V_1^2} \sim \left(\frac{\rho}{\rho_s - \rho}\right) (C_d)^{2/3} \left(\frac{a}{d}\right)^{2/3}. \tag{2.8}$$

Equation (2.8) shows that the scour depth of equilibrium, normalized with the kinetic head of the undisturbed approach flow, depends on the specific gravity of the sediment (i.e. $\rho/(\rho_s - \rho)$), a drag coefficient (i.e. C_d), and the so-called relative coarseness (i.e. a/d). According to the literature (Ranga Raju *et al.* 1983; Qi, Eames & Johnson 2014), the drag coefficient of cylinders impinged by open-channel flows depends on the cylinder shape, the blockage ratio (i.e. a/B, where B is the channel width), the ratio between flow depth and cylinder diameter (i.e. y_1/a), the Froude number of the impinging flow (i.e. $Fr = V_1/\sqrt{g y_1}$), and the cylinder Reynolds number (i.e. $Re = V_1 a/\nu$, where ν is the kinematic fluid viscosity). The dependence of C_d on Re is probably weak because of the turbulent nature of most open-channel flows, both in the laboratory and in the field.

2.3. *Live-bed conditions*

For the clear-water case, the equilibrium condition (i.e. the incipient motion condition) $\tau \approx \tau_c$ was used to derive a predictive formula for the maximum scour depth. For the live-bed case the equilibrium condition is different, as it involves a balance between the time-averaged flux of sediment transported within the scour hole, i.e. Q_{in}, and the time-averaged flux of sediment removed, i.e. Q_{out} (Melville 1984) (averages must be taken over time scales much larger than those associated with the passage of bed forms). Therefore, the equilibrium condition for live-bed scour is $Q_{in} = Q_{out}$. Unfortunately, this condition cannot be further developed to derive a formula for y_s because of the difficulties in theoretically predicting sediment fluxes that occur within the scour hole (i.e. Q_{out}), which is characterized by a complex geometry and flow. However, the following arguments can be used to find a solution to the problem.

We start by pointing out that most of Q_{in} must be in the form of bed-load because most of the sediment fluxes entering within the scour hole must occur next to the bed. Furthermore, most of (if not all) the laboratory experiments on live-bed scour that are available from the literature were carried out with bed-load only and hence we restrict our analysis to this transport regime. From the theory of sediment transport, the dimensionless bed-load sediment discharge per unit channel width (i.e. q_s^*) is commonly estimated through power laws of the type

$$q_s^* = \alpha \left(\tau^* - \tau_c^*\right)^n, \tag{2.9}$$

where $q_s^* = q_s/\{d\sqrt{dg[(\rho_s - \rho)/\rho]}\}$, q_s is the dimensional sediment volumetric discharge per unit channel width, τ^* is the so-called Shields parameter defined as the ratio between the shear stress in the undisturbed bed and the critical shear stress of sediment τ_c; τ_c^*, α and n are constants (see e.g. Yang 1996). Since shear stresses and depth-averaged velocities in the undisturbed channel can be related through a friction factor (i.e. $\tau = (\rho V_1^2 f)/8$, where f is the Darcy–Weisbach friction factor), q_s^* can also be estimated as a function of $(V_1/V_c)^2$, where V_c is the critical velocity for the sediment and V_1/V_c is commonly referred to as the flow intensity parameter (Yang 1996).

The hypotheses and the arguments underpinning the derivation of the shear stress formula for the clear-water case (see (2.6)) are also applicable to live-bed conditions. It is now easy to show that, at equilibrium, the scour depth function S_e, defined as

$$S_e = \frac{y_s g}{V_1^2} \Bigg/ \left[\left(\frac{\rho}{\rho_s - \rho}\right)(C_d)^{2/3}\left(\frac{a}{d}\right)^{2/3}\right], \tag{2.10}$$

represents the ratio between the critical shear stress (i.e. $\tau_c \sim (\rho_s - \rho)gd$) and the shear stress acting at the point of maximum scour as obtained from (2.6) using $S = y_s$. Equation (2.10) is essentially the inverse of a Shields parameter. In live-bed conditions, S_e must depend on the sediment discharge in the undisturbed flow. Since S_e is effectively the inverse of a local Shields parameter, its value at equilibrium should depend on q_s rather than on Q_{in}, which is an integral quantity that includes contributions of sediment fluxes from flow regions away from the point of maximum scour that do not contribute to the local sediment mass balance. Since q_s is essentially dictated by V_1/V_c (or τ^*: see (2.9)), we assume that in live-bed conditions the dimensionless scour depth is related to V_1/V_c by the equation

$$S_e = \phi\left\{V_1/V_c\right\}, \tag{2.11}$$

where the functional relation ϕ must be found experimentally. We have chosen to use V_1/V_c instead of τ^* because, for validation purposes, V_1/V_c is readily available from the literature reporting live-bed scour experiments, unlike τ^*.

3. Validation

3.1. *Clear-water conditions*

The validation of (2.8) is carried out by using experimental data for the case of cylindrical structures with circular cross-section, uniform sediment beds and steady, turbulent shear flows. Data of this kind are largely available from the literature.

The linear dependence of $(y_s g)/V_1^2$ on $\rho/(\rho_s - \rho)$ cannot be tested because this parameter is practically constant in most of the available experiments. Similar difficulties apply to testing the scaling derived for C_d because, in general, C_d values are contained within a range that is too small to test the occurrence of a power law with confidence. Instead, the proposed scaling for the relative roughness a/d can be extensively validated from experimental data. To this end it is important to further clarify under which conditions (2.8) is applicable. Equation (2.8) was derived under the assumption that the sediment diameter is within the range of length scales pertaining to the inertial range, i.e. $\eta \ll d \ll S$. At equilibrium, this condition becomes $\eta \ll d \ll y_s$. In order to find predictive conditions at which (2.8) can be applied, it is necessary to replace y_s, which is not known *a priori*, with a known parameter that is of the same order of magnitude as y_s. It is well known from the literature that y_s scales well with a, more precisely $a < y_s < 3a$ (see e.g. Lee & Sturm 2009). Assuming $y_s \approx a$, the TKE production can be estimated from (2.4) as $\epsilon \sim (C_d V_1^3)/a$, and hence the order of magnitude of the bulk Kolmogorov length scale can be estimated as

$$\eta \sim \left(\frac{\nu^3}{\epsilon}\right)^{1/4} \sim \left(\frac{\nu^3 a}{C_d V_1^3}\right)^{1/4}, \tag{3.1}$$

and therefore, (2.8) is valid if

$$\left(\frac{\nu^3 a}{C_d V_1^3}\right)^{1/4} \ll d \ll a, \tag{3.2}$$

or, analogously, if

$$1 \ll \frac{a}{d} \ll C_d^{1/4} Re^{3/4}. \tag{3.3}$$

Owing to the small exponent of the drag coefficient, it is fair to assume that $C_d^{1/4} \approx 1$, and therefore the range of validity of the proposed theory can be expressed as

$$1 \ll \frac{a}{d} \ll Re^{3/4}. \tag{3.4}$$

Since it was assumed that $S \sim y_s \approx a$, a/d can now be physically interpreted as the ratio between characteristic scales associated with energy containing eddies (i.e. a) and roughness elements (i.e. d) within the scour hole.

The validity of (2.8) is now tested against the laboratory data provided by Ettema (1980), Sheppard *et al.* (2004), Ettema, Kirkil & Muste (2006) and Lança *et al.* (2013). This data set is also utilized to further constrain the limits of validity of the proposed theory as expressed by (3.4).

Table 1 provides a summary of the relevant experimental conditions associated with each referenced source. The definition of equilibrium scour depth is, in general, arbitrary and not consistent over these four studies: in the experiments by Ettema (1980) and Ettema *et al.* (2006) equilibrium conditions were considered to be reached when no appreciable change of the maximum depth was observed over a minimum

Source	a/B	y_1/a	Fr_a	a/d	Fr	$Re \times 10^4$
Ettema *et al.* (2006)	0.02–0.13	2.5–15.6	0.30–0.58	61–387	0.15	3–19
Lança *et al.* (2013)	0.02–0.91	0.5–5.0	0.10–0.47	58–4155	0.07–0.38	1–43
Ettema (1980)	0.02–0.15	0.2–21.0	0.17–2.53	4–1000	0.07–1.00	1–26
Sheppard *et al.* (2004)	0.01–0.15	0.19–11.5	0.10–0.39	136–414	0.07–0.38	3.2–69
	V_1 (m s^{-1})	a (m)	d (mm)	y_1 (m)		
Ettema *et al.* (2006)	0.46	0.06–0.4	1.00	1.00		
Lança *et al.* (2013)	0.27–0.47	0.05–0.91	0.22–0.86	0.05–1.81		
Ettema (1980)	0.18–1.34	0.02–0.24	0.24–7.8	0.02–0.60		
Sheppard *et al.* (2004)	0.29–0.70	0.11–0.91	0.22–2.9	0.17–1.90		

TABLE 1. Range of experimental data pertaining to clear-water scour experiments extracted from the literature: a is the cylinder diameter, V_1 is the depth-averaged velocity, B is the channel width, y_1 is the flow depth, $Fr_a = V_1/\sqrt{ga}$ is the cylinder Froude number, $Fr = V_1/\sqrt{gy_1}$ is the Froude number of the flow, d is the sediment diameter, and $Re = V_1 a/\nu$ is the cylinder Reynolds number. The majority of the experiments reported by Lança *et al.* (2013) were carried out using $V_1 = 0.3$ m s^{-1} and $d = 0.86$ mm, with only four experiments varying these parameters within the range reported in this table. All the experiments were carried out using uniform quartz sand of density $\rho_s = 2650$ kg m^{-3}.

period of four hours. Instead Sheppard *et al.* (2004) and Lança *et al.* (2013) applied the concept of equilibrium as an asymptotic condition, as discussed in § 2.1. In order to avoid fictitious scatter of data, the validity of the proposed scaling for a/d is tested by plotting $y_s g/V_1^2$ versus a/d for each data set individually (figure 4).

Before commenting on figure 4 we further discuss the uncertainties associated with the assumptions underpinning the proposed theory in relation to the experimental data reported in table 1. Equation (2.8) was derived under the assumption of fully rough conditions and hence it was possible to assume that, at equilibrium, the critical shear stress scaled as $\tau_c \sim (\rho_s - \rho)gd$ and the shear stress τ had only a turbulent component (see (2.3)). Fully rough conditions are typical of flows over gravel beds or coarse sands (Shields 1936; Buffington & Montgomery 1997). However, sediment diameters reported in table 1 mostly pertain to sand beds, for which the transitionally rough regime is more likely to occur at equilibrium conditions. In principle, for such a regime, the proposed scaling for both τ_c and τ does not hold, because both shear stresses should also depend upon viscosity. Ignoring viscosity effects, therefore, introduces some uncertainty, which is discussed in the following two points. (i) According to the pioneering work of Shields on sediment entrainment, viscosity effects in transitionally rough flows can account for variations of $\tau_c/(\rho_s - \rho)gd$ (i.e. the Shields parameter) contained within a range of $\pm 33\,\%$ (Shields 1936; Buffington & Montgomery 1997) around an intermediate value. (ii) Similarly, according to the seminal work of Nikuradse on turbulent flows over granular walls, within the transitionally rough regime and for a given relative roughness, viscosity effects can account for variations of friction factors (and hence of bed shear stress τ) contained within a range of $\pm 10\,\%$ (Yang & Joseph 2009) around an intermediate value.

Some uncertainty is also introduced by the drag coefficient C_d. In order to isolate the effects of a/d on $y_s g/V_1^2$, we discarded all the experimental data associated with flow conditions that could include significant variations in C_d. In particular, all the experiments characterized by $y_1/a < 1.4$ were discarded, because for these cases

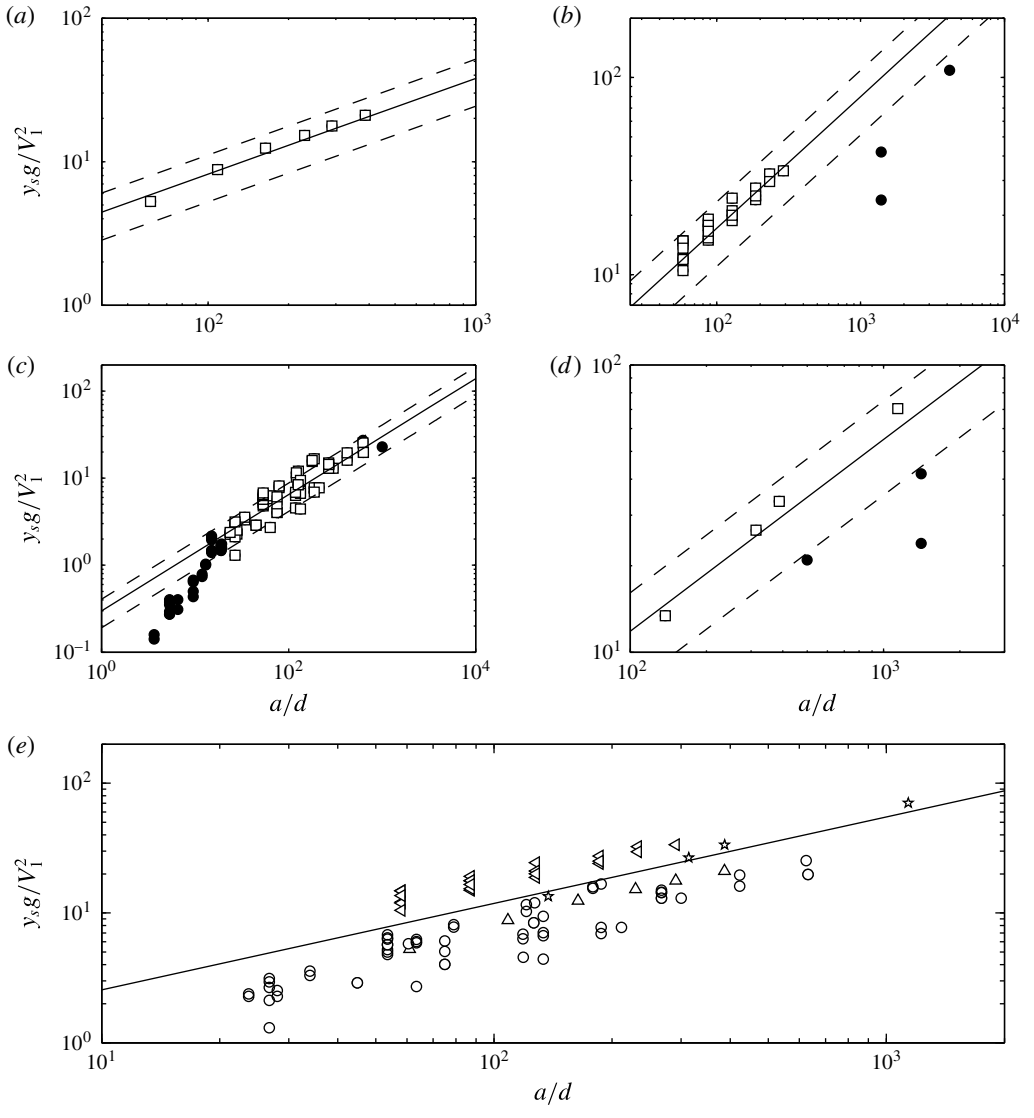

FIGURE 4. Dimensionless scour depths versus relative coarseness: (*a*) data from Ettema *et al.* (2006); (*b*) data from Lança *et al.* (2013); (*c*) data from Ettema (1980); (*d*) data from Sheppard *et al.* (2004). For (*a–d*) white squares and black circles refer to values of a/d that are within and outside the limits imposed by (3.5), respectively. In these panels the solid lines represent a 2/3 power law that best fits the white squares, whereas dashed lines represent the associated $\pm 36\,\%$ error lines. (*e*) All the experimental points contained within the limits imposed by (3.5) are plotted together to provide a general overview: vertical triangles, Ettema (1980); left-pointing triangles, Sheppard *et al.* (2004); circles, Ettema *et al.* (2006); stars, Lança *et al.* (2013). In (*e*) the solid line represents a power law with a 2/3 exponent.

the surface roller interacts with the near-wall horseshoe vortex and therefore it is likely to alter significantly the drag coefficient of the cylinder and consequently the equilibrium scour depth (Melville & Coleman 2000). All the remaining experiments

were characterized by flow conditions with blockage ratio and Froude numbers which, according to Ranga Raju *et al.* (1983), induce variations of bulk drag coefficients C_d of $\pm 15\,\%$. This means that assuming a constant C_d in (2.8) introduces a relative error of $\pm 10\,\%$ on $C_d^{2/3}$.

Combining the relative errors of C_d, τ_c and τ in (2.8) implies that $y_s g/V_1^2$ can be estimated with a maximum relative error of about $\pm 36\,\%$, with τ_c providing the largest contribution.

Figure 4 illustrates $y_s g/V_1^2$ as a function of a/d in log–log plots for all data sets. The figure shows that, for each data set, a/d varies over at least one order of magnitude and hence the proposed power-law scaling for a/d (dashed line in figure 4) can be validated with confidence. Overall, figure 4 shows that the majority of the experimental data pertaining to intermediate values of a/d agree well with the proposed theory.

The experimental data are now used to better constrain the lower and higher bounds of the intermediate range of a/d values identified by (3.4) which, in turn, identifies the limits of validity of the proposed theory. The lower bound can be found from the data by Ettema (1980) (figure 4*c*), which shows that the 2/3 scaling holds for $a/d > 20$. Below this threshold the theory over-predicts the normalized scour depth. In fact, when $a/d < 20$, there is poor scale separation between roughness elements and large eddies of the flow. Therefore, d becomes comparable to the energy-containing eddies and, with respect to the case of d belonging to the inertial range, the flow resistance offered by the roughness elements is enhanced. In other words, the effective roughness of the scour hole increases and therefore y_s decreases. The phenomenon of enhanced effective roughness of rough-walled flows with poor scale separation is well known in hydraulics (see e.g. Chow 1988). For example, when the scale separation between flow depth and roughness (i.e. y_1/d) is not large enough, Manning's coefficients of rough beds underlying turbulent open-channel flows increase with decreasing y_1/d (see e.g. Ferguson 2010). The flow depth y_1 and the cylinder diameter a quantify the scale of energy-containing eddies in open-channel flows and flows around cylinders, respectively. Therefore, for both flow types the ratios y_1/d and a/d have the same physical meaning. Interestingly, and consistent with the results reported herein, Ferguson (2010) shows that Manning's coefficient begins to be influenced by the relative submergence for $y_1/d < 20$.

The data from Sheppard *et al.* (2004) and Lança *et al.* (2013) help to identify the upper bound in (3.4), which is Reynolds-number-dependent and therefore cannot be visually found from figure 4. The data points not respecting the proposed 2/3 scaling are associated with experimental conditions for which the sediment diameter was less than five times the Kolmogorov length scale (i.e. for $d/\eta < 5$), as estimated with (3.1). In wall turbulence, η is closely related to the viscous length scale of the flow (see figure 3 and Gioia & Chakraborty 2006) and therefore, if $d/\eta < 5$, sediment grains are likely to be of a size comparable to the viscous sublayer thickness. This, in turn, means that the shear stress at the water–sediment interface becomes predominantly viscous, so the eddies of size d no longer dominate the turbulent momentum transfer (figure 3) and hence the proposed theory no longer holds. Furthermore, figure 4 shows that all the data points for which $d/\eta < 5$ are associated with values of $y_s g/V_1^2$ that are smaller than those predicted by the 2/3 power law. This is to be expected because the viscous sublayer shelters the sediment grains from the turbulent fluctuations of the flow above and therefore reduces their erosive power.

The upper bound of (3.4) can therefore be identified from the condition $d/\eta > 5$, which, in terms of bulk Reynolds number and relative coarseness, corresponds to

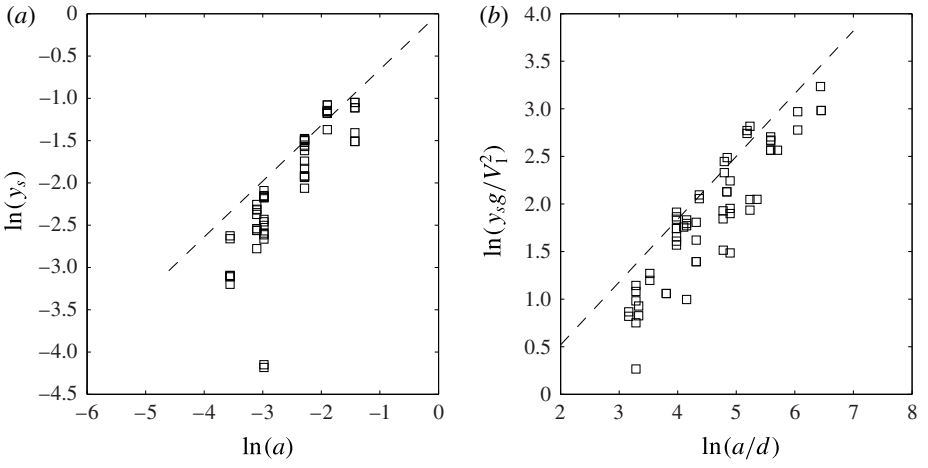

FIGURE 5. Comparison between scaling laws pertaining to y_s versus a (a) and $y_s g/V_1^2$ versus a/d (b). The dashed lines represent a power law with a 2/3 exponent. Data from Ettema (1980).

$a/d < 0.2Re^{3/4}$. It is concluded that (2.8) is valid under the following approximate conditions:

$$20 < \frac{a}{d} < 0.2Re^{3/4}. \tag{3.5}$$

The data of Ettema *et al.* (2006), which are all contained within this range, agree very well with our proposed theory.

Excluding the data points outside the limits imposed by (3.5) leads to a striking agreement between theory and experiments (see figure 4). Furthermore, the $\pm 36\,\%$ error bounds, predicted by the uncertainty analysis presented previously, correspond to the level of scatter appearing in figure 4(*a–d*).

One might argue that the good agreement between theory and experimental data, as reported above, could be the result of a fortuitous correlation between y_s and a. This is because, as already discussed and well reported in the literature, these two parameters are strongly correlated in local scour experiments. To remove this suspicion and further substantiate the validity of the proposed approach, we show that y_s and a display a scaling relation but the associated exponent is different from 2/3. To this end we first note that the experiments by Ettema *et al.* (2006) and Lança *et al.* (2013) were carried out with a weak variation in d and V_1 while the cylinder diameter a was varied extensively (see table 1). This means that plotting $y_s g/V_1^2$ versus a/d taken from these data sets is essentially the same as plotting y_s versus a, and therefore they cannot be used to validate our approach. Instead, the data sets by Ettema (1980) and Sheppard *et al.* (2004) were obtained by extensively varying V_1, d and a. However, only Ettema (1980) provides enough points within the limits imposed by (3.5) to perform a robust statistical analysis (see figure 4*c,d*).

Figure 5 shows the data from Ettema (1980) plotted as y_s versus a (a) and $y_s g/V_1^2$ versus a/d (b) together with a line corresponding to a power law with exponent equal to 2/3. For both panels a best-fit analysis was carried out by minimizing least-squares errors over both the x- and y-coordinate. The best fit of y_s versus a resulted in exponents equal to 0.94 (minimizing errors over the y-coordinate) and 1.1 (minimizing errors over the x-coordinate), which suggests a linear rather than

Source	a/B	y_1/a	Fr_a	a/d	Fr	$Re \times 10^4$
Chiew (1984)	0.07–0.12	3.3–7.6	0.35–2.80	10–186	0.17–1.25	0.8–8.3
Sheppard & Miller (2006)	0.14	1.3–3.2	0.14–1.77	181–563	0.08–1.26	2.6–33
	V_1 (m s^{-1})	a (m)	d (mm)	y_1 (m)	V_c (m s^{-1})	
Chiew (1984)	0.22–1.84	0.03–0.05	0.24–3.20	0.17–0.34	0.27–0.73	
Sheppard & Miller (2006)	0.17–0.21	0.15	0.27–0.84	0.3–0.43	0.25–0.4	

TABLE 2. Range of experimental data pertaining to live-bed scour experiments extracted from the literature: V_c is the critical velocity for sediment; all the other symbols are as in table 1.

power-law relation between the two variables. Instead, the best fit of $y_s g/V_1^2$ versus a/d resulted in exponents equal to 0.67 (minimizing errors over the y-coordinate) and 0.81 (minimizing errors over the x-coordinate), which are reasonably close to the theoretically predicted value of $2/3 \approx 0.67$. We therefore conclude that the proposed scaling is not the result of a fortuitous correlation between y_s and a.

3.2. *Live-bed conditions*

In live-bed conditions the proposed theory essentially suggests that if scour depth function S_e is plotted against the flow intensity parameter V_1/V_c, experimental data should collapse around a curve identified by a functional relation ϕ (see (2.11)). In order to substantiate these hypotheses, experimental data were extracted from Chiew (1984) and Sheppard & Miller (2006) for a total of 167 data points. As in the clear-water case, these experiments were carried out with circular cylinders and uniform quartz sand. Only very few data points with $y_1/a < 1.4$ were filtered out. Table 2 provides a summary of the relevant experimental data, which include a wide range of hydraulic conditions.

Since in live-bed conditions the maximum scour depths oscillate in time due to the passage of bed-forms, here y_s is taken as the time-averaged value of maximum scour depths as reported by the authors of the referenced papers. Contrary to the clear-water case, in live-bed conditions there is no ambiguity about the definition of y_s, so the proposed theory can be tested against all data sets at once and not for each data set individually.

Figure 6 shows that the agreement between theory and experiments is striking. The experimental data, with exception of a few points, collapse nicely onto a power-law function of the type

$$\phi = \beta \left(\frac{V_1}{V_c} \right)^{\theta}, \tag{3.6}$$

with $\beta = 0.47$ and $\theta = -1.89$. Interestingly, the points that do not collapse on (3.6) are associated with $a/d < 20$. This suggests that, although (3.5) was obtained from the analysis of experimental data pertaining to clear-water flows, it seems to be applicable to live-bed flows as well. Furthermore, consistent with the clear-water case, for these experimental points the proposed theory over-predicts scour depths. As discussed earlier, this is an effect associated with an increase in flow resistance due to the poor scale separation between sediment diameter and energy-containing eddies.

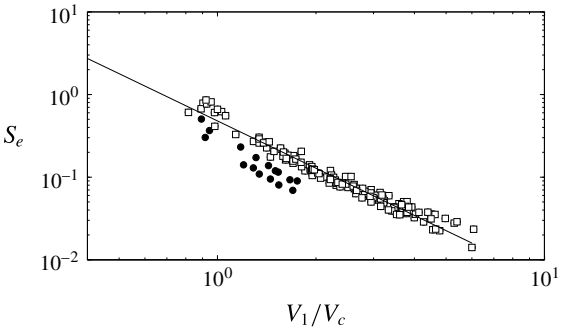

FIGURE 6. S_e versus the flow intensity parameter V_1/V_c. Experimental data are taken from Chiew (1984) and Sheppard & Miller (2006). White squares and black circles refer to values of a/d that are within and outside the limits imposed by (3.5), respectively. The solid line is the best fit to the white square data (see (3.6)).

4. Discussion and conclusion

We now discuss how the proposed theory relates to the dimensional arguments commonly applied in the literature pertaining to local scour around bridge piers. Various authors argue that for the case of circular cylinders, uniform sediment and steady conditions (i.e. the conditions investigated herein) the scour depth of equilibrium, normalized as y_s/a, depends on the following set of non-dimensional groups (see e.g. Ettema, Melville & Barkdoll 1998; Ettema *et al.* 2011):

$$\frac{y_s}{a} = \Phi_1 \left\{ \frac{a}{B}; \frac{y_1}{a}; Fr_a; \frac{a}{d}; \frac{V_1}{V_c}; Re; \frac{\rho_s}{\rho} \right\}, \tag{4.1}$$

where $Fr_a = V_1/\sqrt{ga}$ is the cylinder Froude number. All the non-dimensional groups listed above stem naturally from the application of dimensional arguments and of the Buckingham-Π theorem, except for V_1/V_c, which is somewhat artificially included (Simarro, Teixeira & Cardoso 2007) because it has the important physical meaning of identifying the cross-over between clear-water (i.e. $0.5 \leqslant V_1/V_c \leqslant 1$) and live-bed conditions (i.e. $V_1/V_c > 1$).

Dividing both sides of (2.8) by a gives

$$\frac{y_s}{a} \sim (Fr_a)^2 \left(\frac{\rho}{\rho_s - \rho} \right) (C_d)^{2/3} \left(\frac{a}{d} \right)^{2/3}, \tag{4.2}$$

which is valid for clear-water conditions.

For live-bed conditions the formula for the scour depth of equilibrium is

$$S_e = \frac{y_s g}{V_1^2} \Big/ \left[\left(\frac{\rho}{\rho_s - \rho} \right) (C_d)^{2/3} \left(\frac{a}{d} \right)^{2/3} \right] = \phi \{V_1/V_c\}. \tag{4.3}$$

Dividing (4.3) by a gives

$$\frac{y_s}{a} \sim \phi \left\{ \frac{V_1}{V_c} \right\} (Fr_a)^2 \left(\frac{\rho}{\rho_s - \rho} \right) (C_d)^{2/3} \left(\frac{a}{d} \right)^{2/3}, \tag{4.4}$$

where ϕ is given by (3.6).

It is now evident that the proposed approach allows the derivation of two equations that naturally contain all the non-dimensional groups identified by dimensional arguments and clarify their effects from a physical point of view. All such groups appear explicitly in (4.2) and (4.4), with the exception of a/B, y_1/a and Re. However, the effects of the first two are lumped into the drag coefficient C_d (which, according to the relevant literature, may also be dependent on Fr and, weakly, on Re) and are therefore associated with momentum transfer mechanisms occurring between the fluid and the cylinder. With the exception of very few studies (Ettema *et al.* 2006; Simarro *et al.* 2007), the effects of Re are commonly neglected in the literature providing formulas for local scour prediction (see e.g. Ettema *et al.* 1998; Lee & Sturm 2009). We have shown that such effects are, instead, rather important since Re, in conjunction with the relative coarseness a/d, dictates the nature of momentum transfer mechanisms at the sediment–water interface and ultimately influences the magnitude of the equilibrium scour depth. In particular, it was shown that if $20 < a/d < 0.2Re^{3/4}$, then $y_s g/V_1^2 \sim (a/d)^{2/3}$. Such a clean scaling is lost when $a/d > 0.2Re^{3/4}$ and $a/d < 20$, due to viscous sheltering and increased flow resistance effects, respectively.

Again, the main objective of the present paper is not to propose yet another formula for direct applications in engineering. The aim is, rather, to propose a novel approach that combines theoretical arguments with considerations taken from empirical evidence, to develop a better understanding of the physics of local scouring around structures, and therefore to provide new avenues for the development of general predictive models that are founded more on physical than empirical grounds.

Acknowledgements

The authors would like to thank Dr M. Postacchini and Professor A. Marion for fruitful discussions. The comments proposed by four anonymous reviewers helped to significantly improve the clarity of the paper. C.M. also acknowledges Network Rail (ref. no. SU009) for partly funding this research. The work was finalized when C.M. was a Campus World Visiting Researcher at the DICEA, Università Politecnica delle Marche. M.B. acknowledges support by (i) the Italian RITMARE Flagship Project (SP3-WP4), a National Research Programme funded by the Italian Ministry of University and Research, and (ii) the ONR Global (UK), through the NICOP Research Grant (N62909-13-1-N020).

REFERENCES

BOMBARDELLI, F. A. & GIOIA, G. 2006 Scouring of granular beds by jet-driven axisymmetric turbulent cauldrons. *Phys. Fluids* **18**, 088101.

BUFFINGTON, J. M. & MONTGOMERY, D. R. 1997 A systematic analysis of eight decades of incipient motion studies, with special reference to gravel-bedded rivers. *Water Resour. Res.* **33** (8), 1993–2029.

CHIEW, Y. M. 1984 Local scour at bridge piers. PhD thesis, Department of Civil Engineering, University of Auckland, Auckland, New Zealand.

CHOW, V. T. 1996 *Open Channel Hydraulics*. McGraw-Hill.

ETTEMA, R. 1980 Scour at bridge piers. *Rep.* 216. School of Engineering, The University of Auckland, Auckland, New Zealand.

ETTEMA, R., CONSTANTINESCU, G. & MELVILLE, B. 2011 Evaluation of bridge scour research: pier scour processes and predictions. *NCHRP Rep.* 175.

ETTEMA, R., KIRKIL, G. & MUSTE, M. 2006 Similitude of large-scale turbulence in experiments on local scour at cylinders. *J. Hydraul. Engng* **132** (1), 33–40.

ETTEMA, R., MELVILLE, B. W. & BARKDOLL, B. 1998 Scale effect in pier-scour experiments. *J. Hydraul. Engng* **124** (6), 639–642.

FERGUSON, R. 2010 Time to abandon the Manning equation? *Earth Surf. Proces. Landf.* **35**, 1873–1876.

FRISCH, U. 1995 *Turbulence: The Legacy of A. N. Kolmogorov*. Cambridge University Press.

GIOIA, G. & BOMBARDELLI, F. A. 2002 Scaling and similarity in rough channel flows. *Phys. Rev. Lett.* **88** (1), 014501.

GIOIA, G. & BOMBARDELLI, F. A. 2005 Localized turbulent flows on scouring granular beds. *Phys. Rev. Lett.* **95** (1), 014501.

GIOIA, G. & CHAKRABORTY, P. 2006 Turbulent friction in rough pipes and the energy spectrum of the phenomenological theory. *Phys. Rev. Lett.* **96** (4), 044502.

KNIGHT, B. & SIROVICH, L. 1990 Kolmogorov inertial range for inhomogeneous turbulent flows. *Phys. Rev. Lett.* **65** (11), 1356–1359.

KIRKIL, G., CONSTANTINESCU, G. & ETTEMA, R. 2008 Coherent structures in the flow field around a circular cylinder with scour hole. *J. Hydraul. Engng* **134** (5), 572–587.

KOLMOGOROV, A. N. 1991 The local structure of turbulence in incompressible viscous fluid for very large Reynolds numbers. *Proc. R. Soc. Lond.* A **434**, 9–13.

KOTHYARI, U. C., HAGER, W. H. & OLIVETO, G. 2007 Generalized approach for clear-water scour at bridge foundation elements. *J. Hydraul. Engng* **133** (11), 1229–1240.

LANÇA, R. M, FAEL, C. S., MAIA, R. J., PEGO, J. P. & CARDOSO, A. H. 2013 Clear-water scour at comparatively large cylindrical piers. *J. Hydraul. Engng* **139** (11), 1117–1125.

LEE, S. O. & STURM, T. W. 2009 Effect of sediment size scaling on physical modeling of bridge scour. *J. Hydraul. Engng* **135** (10), 793–802.

MELVILLE, B. 1984 Live-bed scour at bridge piers. *J. Hydraul. Engng* **110** (9), 1234–1247.

MELVILLE, B. W. & CHIEW, Y. M. 1999 Time scale for local scour at bridge piers. *J. Hydraul. Engng* **125** (1), 59–65.

MELVILLE, B. & COLEMAN, S. 2000 *Bridge Scour*. Water Resources Publications.

MOSER, D. R. 1993 Kolmogorov inertial range spectra for inhomogeneous turbulence. *Phys. Fluids* **6** (2), 794–801.

QI, Z. X., EAMES, I. & JOHNSON, E. R. 2014 Force acting on a square cylinder fixed in a free-surface channel flow. *J. Fluid Mech.* **756**, 716–727.

RANGA RAJU, K. G., RANA, O. P. S., ASAWA, G. L. & PILLAI, A. S. N. 1983 Rational assessment of blockage effect in channel flow past smooth circular cylinders. *J. Hydraul. Res.* **21** (4), 289–302.

SADDOUGHI, S. G. 1997 Local isotropy in complex turbulent boundary layers at high Reynolds number. *J. Fluid Mech.* **348**, 201–245.

SADDOUGHI, S. G. & VEERAVALLI, S. V. 1994 Local isotropy turbulent boundary layers at high Reynolds number. *J. Fluid Mech.* **268**, 333–372.

SHEPPARD, D. M. & MILLER, W. JR. 2006 Live-bed local pier scour experiments. *J. Hydraul. Engng* **132** (7), 635–642.

SHEPPARD, D. M., ODEH, M. & GLASSER, T. 2004 Large scale clear-water local pier scour experiments. *J. Hydraul. Engng* **130** (10), 957–963.

SHIELDS, A. 1936 *Application of Similarity Principles and Turbulence Research to Bed-Load Movement*. California Institute of Technology; translated from German.

SIMARRO, G., TEIXEIRA, L. & CARDOSO, A. H. 2007 Flow intensity parameter in pier scour experiments. *J. Hydraul. Engng* **133** (11), 1261–1264.

UNGER, J. & HAGER, W. H. 2007 Down-flow and horseshoe vortex characteristics of sediment embedded bridge piers. *Exp. Fluids* **42**, 1–19.

YANG, C. T. 1996 *Sediment Transport: Theory and Practice*. McGraw-Hill.

YANG, C. T. & JOSEPH, D. D. 2009 Virtual Nikuradse. *J. Turbul.* **10**, 1–28.